Supporting Information

Robust Hollow TiO_2 Spheres for Lithium/Sodium Ion Batteries with Excellent Cycle Stability and Rate Capability

Menglong Yao, Hongkang Wang,* Ruifeng Qian, Tianhao Yao, Jian-Wen Shi, Yonghong Cheng

State Key Lab of Electrical Insulation and Power Equipment, Center of Nanomaterials for Renewable Energy (CNRE), School of Electrical Engineering, Xi'an Jiaotong University, Xi'an 710049, PR China

**Corresponding author. E-mail: hongkang.wang@mail.xjtu.edu.cn*

Table of Contents

Experimental Section

Materials characterization

The microstructures of the products were characterized by scanning electron microscopy (SEM，FEI，Quanta 250F) and (high-resolution) transmission electron microscopy ((HR)TEM, Thermo Fisher, Talos F200X). The phase structures of the products were characterized by X-ray diffraction (XRD) under Cu Ka radiation (k = 1.5418 Å) at 30 kV and 10 mA in the 2θ range of 10-80°. The Raman spectrum was obtained on Renishaw Raman RE01 Microscope with an excitation laser of 633 nm. Brunauere-Emmette-Teller (BET) method was used to analyze the specific surface area and the pore characteristics, and the nitrogen sorption isotherms were obtained by using a Quantachrome Surface Area Analyzer (ASAP 2020 Plus HD88) at 77 K. The elemental composition and chemical state of the products were analyzed by X-ray photoelectron spectroscopy (XPS) using an ESCALAB Xi^+ Thermo Fisher XPS instrument.

Electrochemical measurements

The electrochemical properties of the hollow TiO_2 nanospheres were investigated in CR2025 coin-type half-cells. Firstly, the working electrodes were fabricated by casting a slurry on the copper foil, and the slurry was prepared by mixing the active materials (hollow TiO_2), conductive carbon black (ECP-600JD) and polyvinylidene fluoride (PVDF, HSV900, Arkema) with the weight ratio of 7:2:1 and 1-methyl-2-pyrrolidinone (NMP，C_5H_9NO，99.5%，Macklin) as a solvent. The slurry coated copper foils were then dried under vacuum at 60 ^oC for 12h. The working electrodes were punched into round sheets with a diameter of 14 mm, and the loading amount of the active material was about 1.2±0.2 mg/cm^2. LIB/SIB cells were assembled in Ar-filled glove box (H_2O < 0.1 ppm, O_2 < 0. 1 ppm). For LIBs, the lithium foils were used as the counter electrodes, and Celgard 2400 microporous membranes as the separators. A solution of 1 M $LiPF_6$ in a 1:1:1 of ethylene carbonate (EC), diethyl carbonate (DEC), and ethylmethyl carbonate (EMC) was used as the electrolyte. For SIBs, the sodium foils were used as the counter electrodes, and the Whatman glass microfiber membranes as the separators. 1M $NaClO_4$ in EC/DMC (1:1 in volume) with addition of 5 vol% of fluoroethylene carbonate (FEC) was used as the electrolyte. The galvanostatic discharge-charge tests of LIBs and SIBs were performed on a battery test system (Neware BTS, China). Cyclic voltammetry (CV, in the range of 1.0-3.0 V for LIBs, and 0.01-3.0 V for SIBs) and electrochemical impedance spectroscopy (EIS; 0.01-100kHz) were performed on CHI660 (Chenghua, Shanghai) electrochemical workstation.

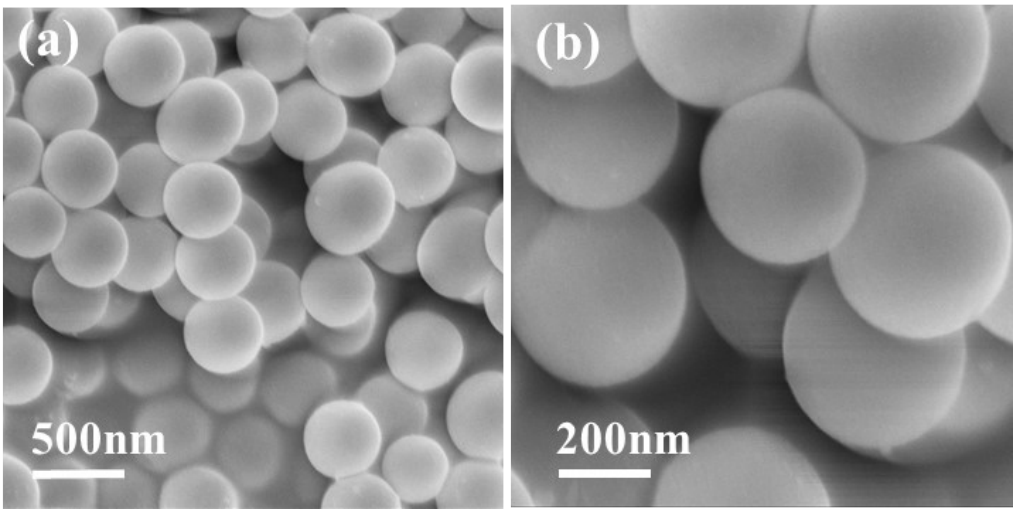

Figure S1. (a, b) SEM images of the as-prepared phenolic resin spheres at different magnification.

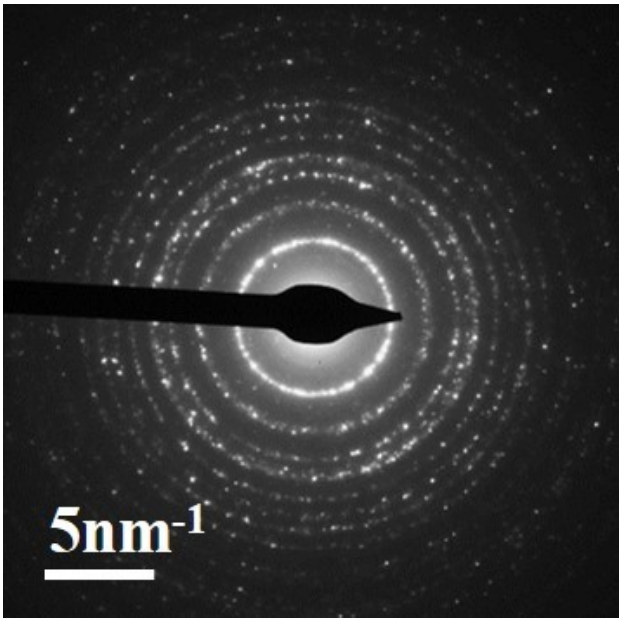

Figure S2. SAED pattern taken on a single TiO_2 hollow sphere.

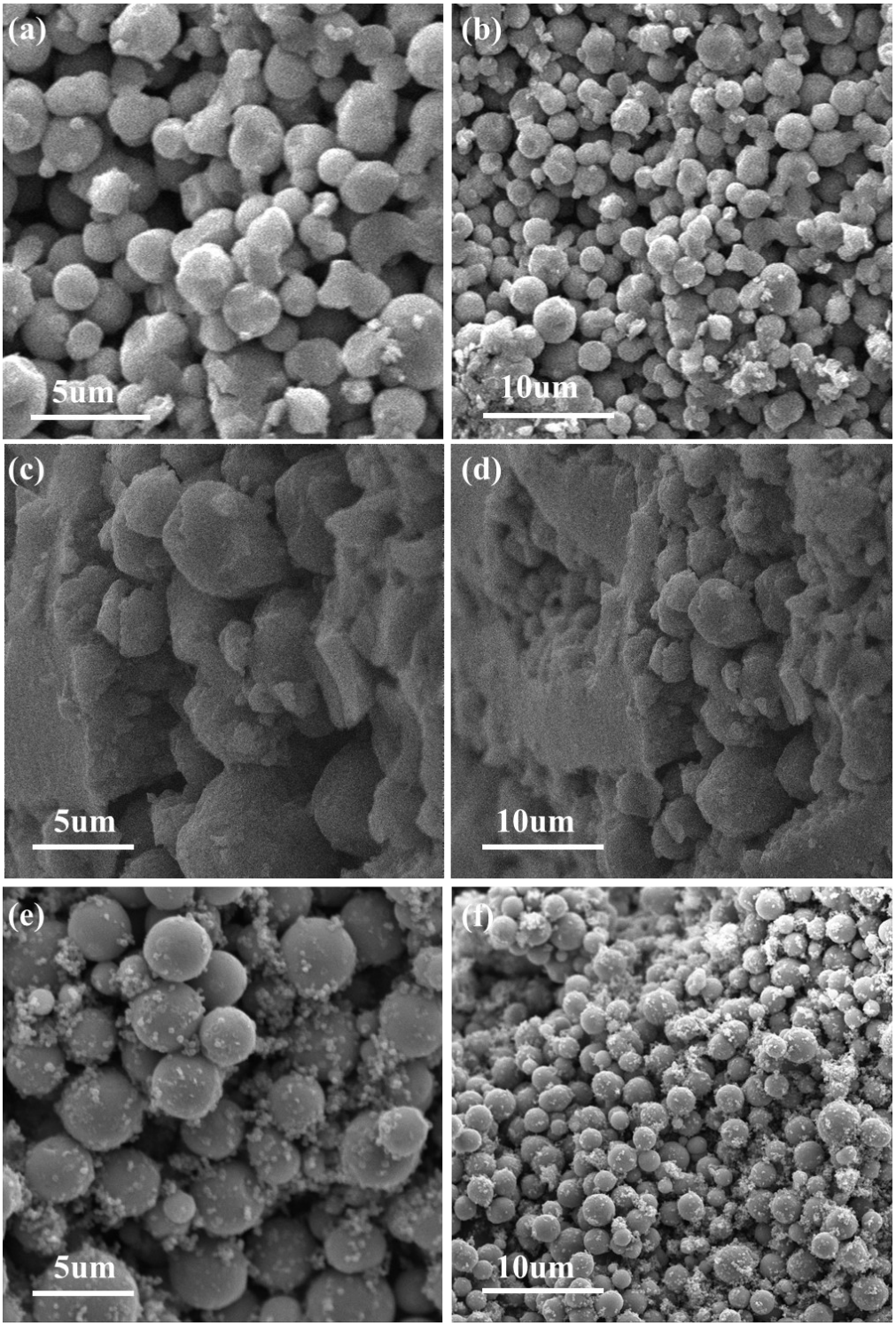

Figure S3. (a-d) SEM images of the TiO_2 prepared without the presence of phenolic resin nanospheres by solvothermal reaction under static (a, b; 0 r/min) and stirring (c, d; 500 r/min) conditions, respectively. (e-f) SEM images of TiO_2 prepared with the presence of phenolic resin nanospheres by solvothermal reaction under static (a, b; 0 r/min). All the products were annealed in air at 600 ^{o}C for 2h.

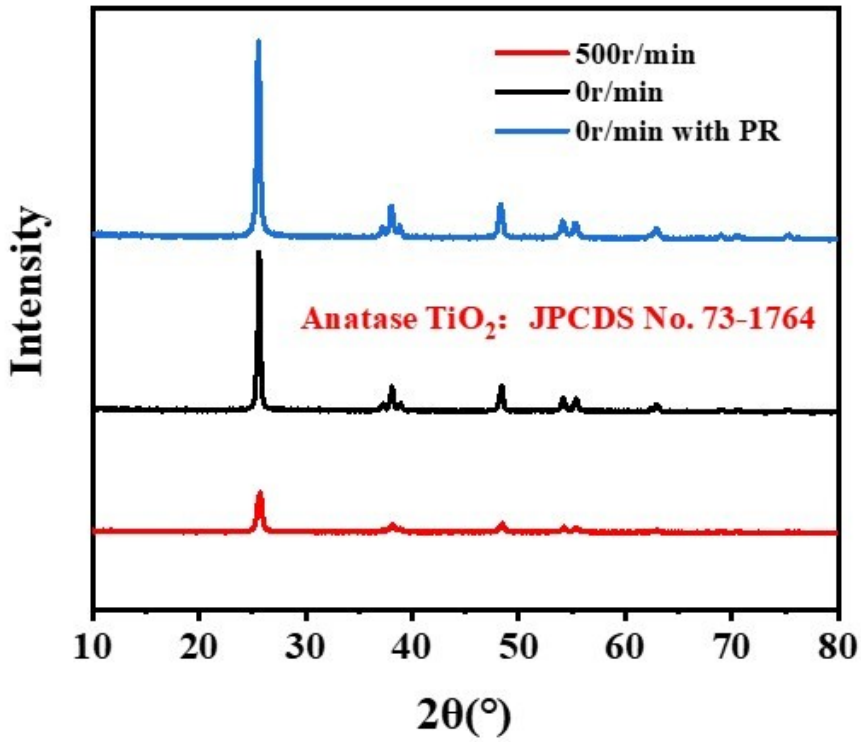

Figure S4. XRD patterns of TiO_2 prepared without/with the presence of phenolic resin nanospheres by solvothermal reaction under static (0 r/min) and stirring (500 r/min) conditions, followed by annealing in air at 600 ^{o}C.

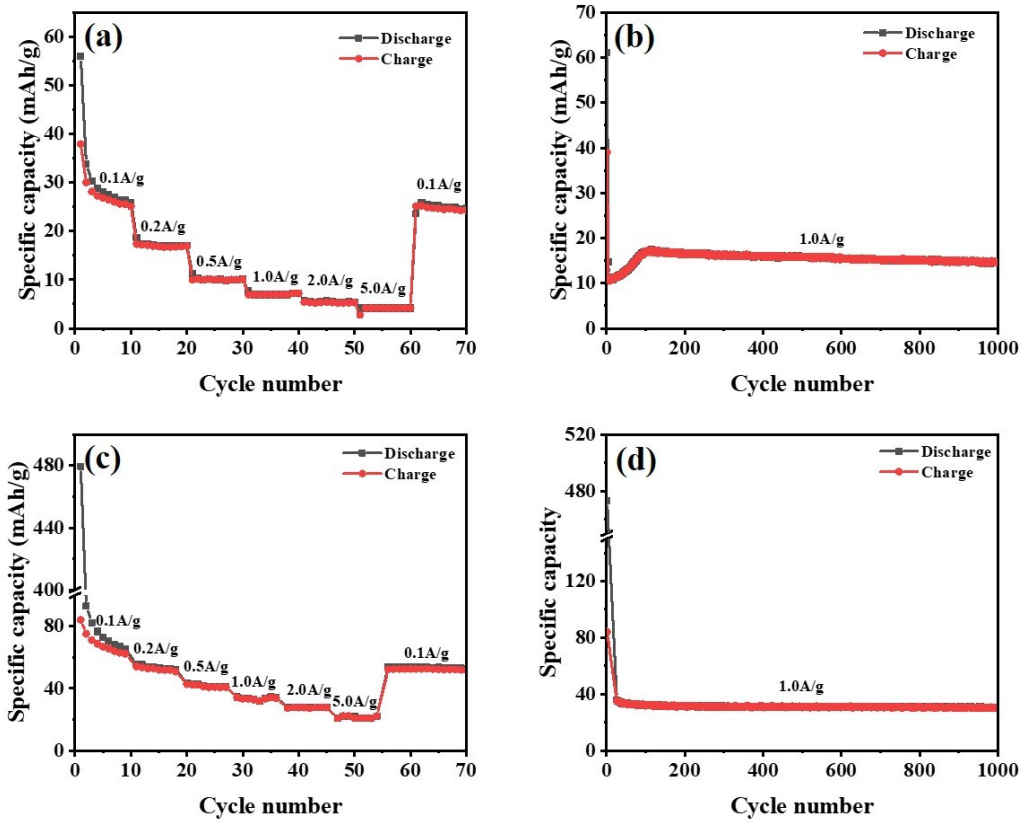

Figure S5. Lithium/Sodium storage behavior of the TiO_2 obtained without the presence of phenolic resin nanospheres by solvothermal reaction under static (0 r/min) condition, followed by annealing in air at 600 ^oC. (a) Rate performance at various current densities and (b) cycle performance at 1.0 A/g for lithium ion batteries. (c) Rate performance at various current densities and (d) cycle performance at 1.0 A/g for sodium ion batteries. For lithium ion batteries, the gradual capacity increases at 1.0 A/g in Figure S3b can be attributed to the electrochemical activation process of TiO_2 anode. [1, 2]

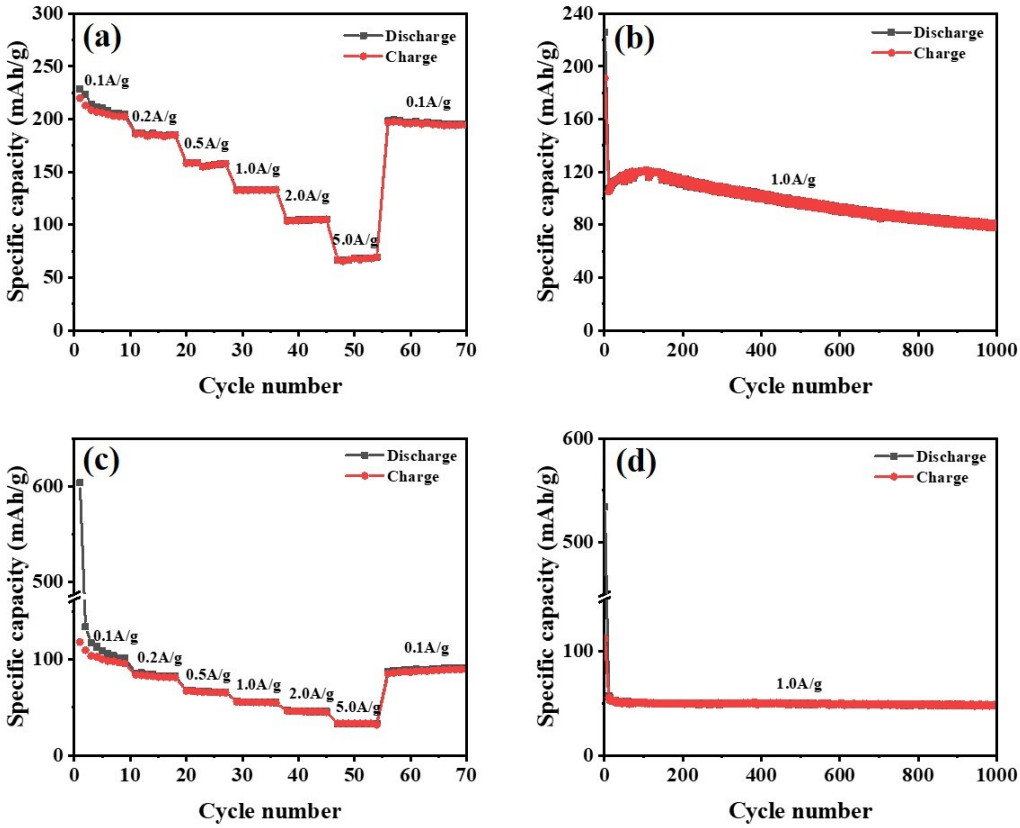

Figure S6. Lithium/Sodium storage behavior of the TiO_2 obtained without the presence of phenolic resin nanospheres by solvothermal reaction under stirring (500 r/min) condition, followed by annealing in air at 600 ^{o}C. (a) Rate performance at various current densities and (b) cycle performance at 1.0 A/g for lithium ion batteries. (c) Rate performance at various current densities and (d) cycle performance at 1.0 A/g for sodium ion batteries.

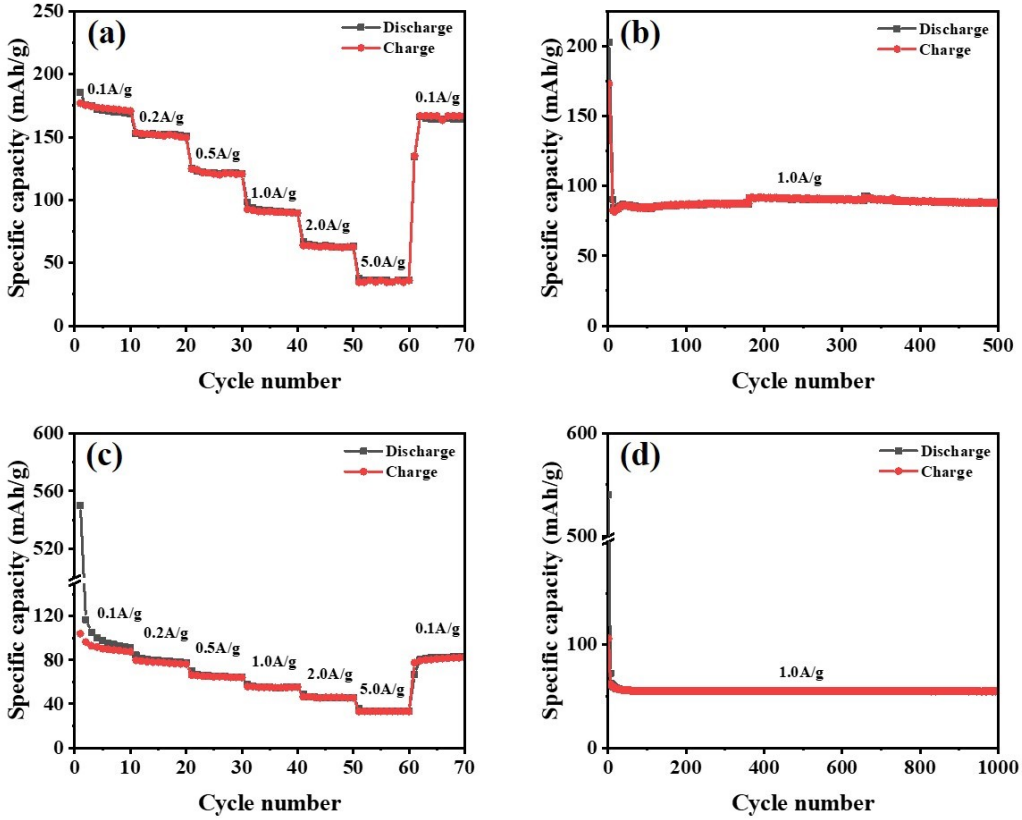

Figure S7. Lithium/Sodium storage behavior of the TiO_2 with the presence of phenolic resin nanospheres by solvothermal reaction under static (0 r/min) condition. (a) Rate performance at various current densities and (b) cycle performance at 1.0 A/g for lithium ion batteries, (c) rate performance at various current densities and (d) cycle performance at 1.0 A/g for sodium ion batteries.

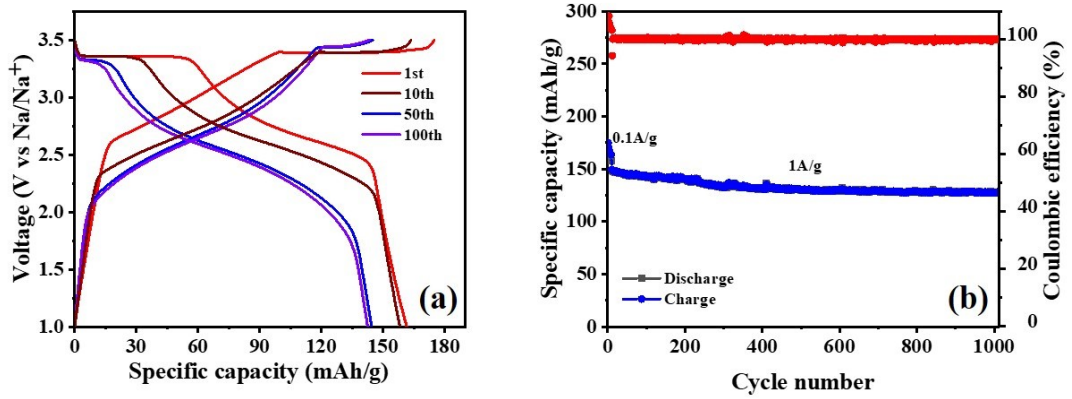

Figure S8. (a-b) Galvanostatic discharge-charge curves of a $TiO_2/Na_3V_2(PO_4)_3$ full-cell cycled at a current density 1.0 A/g in the voltage range of 1-3.5 V, cycle performance at 1.0 A/g of full cell.

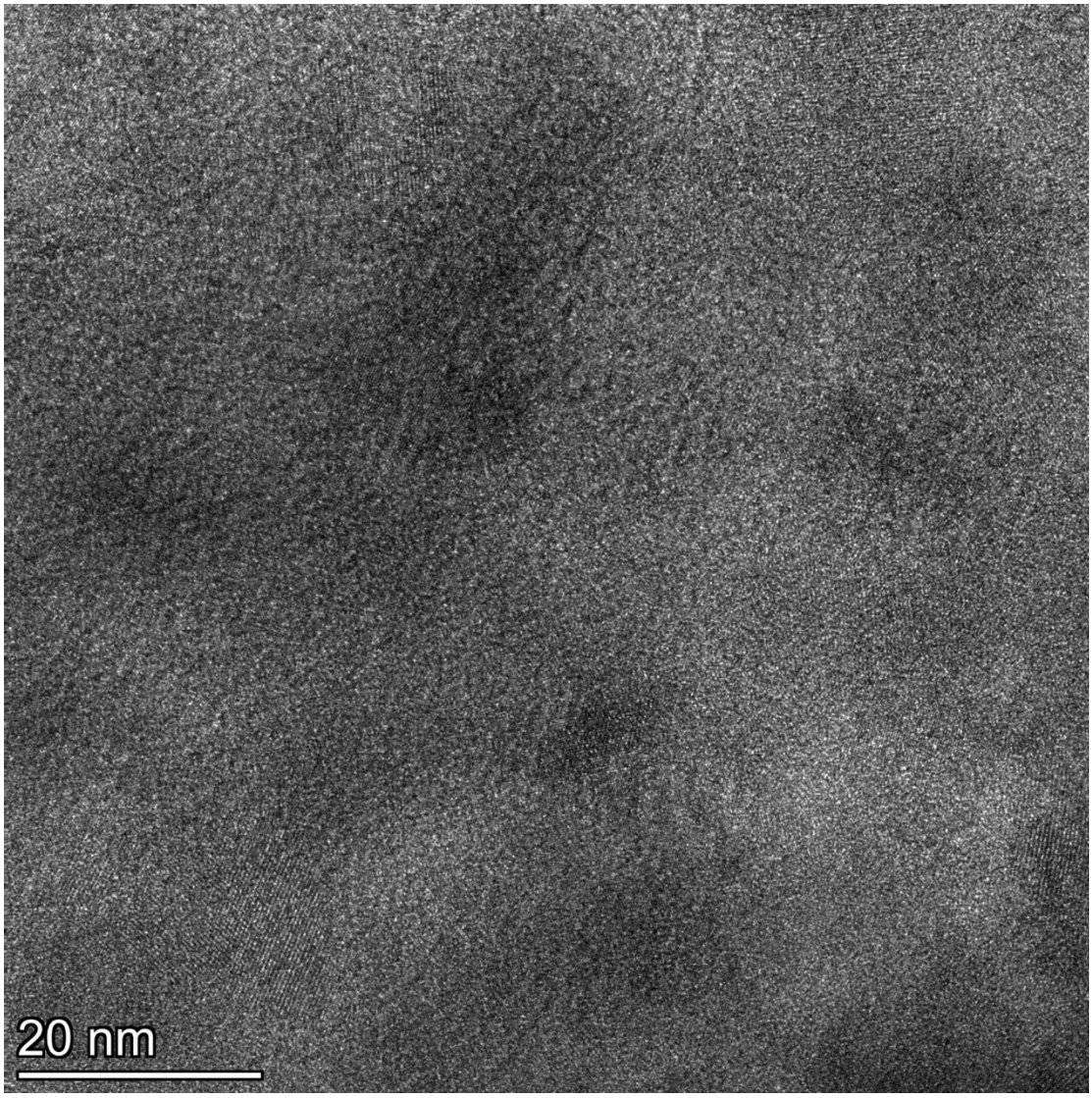

Figure S9. HRTEM image for the charged hollow TiO_2 electrode after 1000 cycles at 1.0 A/g, which shows the crystalline and amorphous regions.

Table S1. Comparison of the lithium storage behavior of various TiO_2 based anode materials.

Materials	Capacity (mAh/g)	Cycle	Current density (mA/g)	Voltage (V vs. Na/Na^+)	Ref.
$TiO_2/C/TiO_2$	237	100	20	1-3	3
TiO_2/C	137	1000	1000	1-3	4
$C/TiO_2/C$	148	1000	1675	1-3	5
Core/Shell TiO_2	151	100	170	1-3	6
TiO_2/Co_3O_4	180	500	300	0-3	7
TiO_2 microboxes	187	300	170	1-3	8
TiO_2 nanowires	173	100	170	1-3	9
Yolk-shell TiO_2	191	40	84	1-3	10
TiO_2 nanotube	180	100	34	1-3	11
TiO_2	**178**	**100**	**200**	**1-3**	**This work**
	138.8	**1000**	**1000**	**1-3**	

Table S2. Comparison of the sodium storage behavior of various TiO_2 based anode materials.

Materials	**Capacity (mAh/g)**	**Cycle**	**Current density (mA/g)**	**Voltage (V vs. Na/Na^+)**	**Ref.**
N/S-TiO_2	90	1000	500	0.02-2	[12]
Fe-TiO_2	127.3	3000	1680	0.001-3	[13]
B-TiO_2	141	400	660	0.01-2.5	[14]
Nb-TiO_2	205	200	50	0.005-3	[15]
Ta-TiO_2	210	300	50	0.005-3	[15]
S-TiO_2	186	100	330	0.01-3	[16]
N/S-TiO_2	120.9	300	1000	0.01-2.5	[17]
Fe-TiO_2	164	1000	1000	0.01-2.5	[18]
Mo-TiO_2	108.3	50	1680	0.01-3	[19]
Nb-TiO_2	169	100	33	0-2.5	[20]
Sn-TiO_2	103	700	5000	0.005-3	[21]
N/C-TiO_2	260.4	300	84	0.01-3	[22]
$TiOF_2$-TiO_2	151.7	2000	500	0.01-3	[23]
Ti_3C_2-TiO_2	153	100	600	0.01-3	[24]
C-TiO_2	125	2500	1000	0.01-3	[25]
N/C/TiF_3-TiO_2	103	1000	1000	0.01-3	[26]
CNTs/C-TiO_2	148	100	100	0.01-3	[27]
TiO_2	**213**	**100**	**200**	**0.01-3**	**This work**
	177	**1000**	**1000**	**0.01-3**	
	115	**4000**	**5000**	**0.01-3**	

References

1. C. Hou, W. Yang, X. Xie, X. Sun, J. Wang, N. Naik, D. Pan, X. Mai, Z. Guo, F. Dang and W. Du, Agaric-like anodes of porous carbon decorated with MoO_2 nanoparticles for stable ultralong cycling lifespan and high-rate lithium/sodium storage, *J. Colloid Inter. Sci.*, 2021, **596**, 396-407.
2. C. Hou, J. Wang, W. Zhang, J. Li, R. Zhang, J. Zhou, Y. Fan, D. Li, F. Dang, J. Liu, Y. Li, K. Liang and B. Kong, Interfacial Superassembly of Grape-Like MnO–Ni@C Frameworks for Superior Lithium Storage, *ACS Appl. Mater. Interfaces*, 2020, **12**, 13770-13780.
3. W. Li, F. Wang, Y. Liu, J. Wang, J. Yang, L. Zhang, A. A. Elzatahry, D. Al-Dahyan, Y. Xia and D. Zhao, General Strategy to Synthesize Uniform Mesoporous TiO_2/Graphene/Mesoporous TiO_2 Sandwich-Like Nanosheets for Highly Reversible Lithium Storage, *Nano Lett.*, 2015, **15**, 2186-2193.
4. H. Liu, W. Li, D. Shen, D. Zhao and G. Wang, Graphitic Carbon Conformal Coating of Mesoporous TiO_2 Hollow Spheres for High-Performance Lithium Ion Battery Anodes, *J. Am. Chem. Soc.* , 2015, **137**, 13161-13166.
5. Y. Zhang, N. Zhang, J. Chen, T. Zhang, W. Ge, W. Zhang, G. Xie, L. Zhang and Y. He, Preparation and lithium storage properties of C@TiO_2/3D carbon hollow sphere skeleton composites, *J. Alloys Compd.*, 2020, **815**, 152511.
6. Y. Cai, H.-E. Wang, X. Zhao, F. Huang, C. Wang, Z. Deng, Y. Li, G. Cao and B.-L. Su, Walnut-like Porous Core/Shell TiO_2 with Hybridized Phases Enabling Fast and Stable Lithium Storage, *ACS Appl. Mater. Interfaces*, 2017, **9**, 10652-10663.
7. D. Zhao, Q. Hao and C. Xu, Nanoporous TiO_2/Co_3O_4 Composite as an Anode Material for Lithium-Ion Batteries, *Electrochim. Acta*, 2016, **211**, 83-91.
8. X. Gao, G. Li, Y. Xu, Z. Hong, C. Liang and Z. Lin, TiO_2 Microboxes with Controlled Internal Porosity for High-Performance Lithium Storage, *Angew. Chem, Int. Ed.*, 2015, **54**, 14331-14335.
9. B. Han, S.-J. Kim, B.-M. Hwang, S.-B. Kim and K.-W. Park, Single-crystalline rutile TiO_2 nanowires for improved lithium ion intercalation properties, *J. Power Sources*, 2013, **222**, 225-229.
10. X. Wang, Y. Wang, L. Yang, K. Wang, X. Lou and B. Cai, Template-free synthesis of homogeneous yolk–shell TiO_2 hierarchical microspheres for high performance lithium ion batteries, *J. Power Sources*, 2014, **262**, 72-78.
11. H. Han, T. Song, E.-K. Lee, A. Devadoss, Y. Jeon, J. Ha, Y.-C. Chung, Y.-M. Choi, Y.-G. Jung and U. Paik, Dominant Factors Governing the Rate Capability of a TiO_2 Nanotube Anode for High Power Lithium Ion Batteries, *ACS Nano*, 2012, **6**, 8308-8315.
12. W. Song, H. Zhao, L. Wang, S. Liu and Z. Li, Co-doping Nitrogen/Sulfur through a Solid-State Reaction to Enhance the Electrochemical Performance of Anatase TiO_2 Nanoparticles as a Sodium-Ion Battery Anode, *ChemElectroChem*, 2018, **5**, 316-321.
13. H. He, D. Sun, Q. Zhang, F. Fu, Y. Tang, J. Guo, M. Shao and H. Wang, Iron-Doped Cauliflower-Like Rutile TiO_2 with Superior Sodium Storage Properties, *ACS Appl. Mater. Interfaces*, 2017, **9**, 6093-6103.

14. B. Wang, F. Zhao, G. Du, S. Porter, Y. Liu, P. Zhang, Z. Cheng, H. K. Liu and Z. Huang, Boron-Doped Anatase TiO_2 as a High-Performance Anode Material for Sodium-Ion Batteries, *ACS Appl. Mater. Interfaces*, 2016, **8**, 16009-16015.
15. H. Usui, Y. Domi, K. Takama, Y. Tanaka and H. Sakaguchi, Tantalum-Doped Titanium Oxide with Rutile Structure as a Novel Anode Material for Sodium-Ion Battery, *ACS Appl. Energy Mater.*, 2019, **2**, 3056-3060.
16. W. Zhang, N. Luo, S. Huang, N.-L. Wu and M. Wei, Sulfur-Doped Anatase TiO_2 as an Anode for High-Performance Sodium-Ion Batteries, *ACS Appl. Energy Mater.*, 2019, **2**, 3791-3797.
17. F. Li, W. Liu, Y. Lai, F. Qin, L. Zou, K. Zhang and J. Li, Nitrogen and sulfur co-doped hollow carbon nanofibers decorated with sulfur doped anatase TiO_2 with superior sodium and lithium storage properties, *J. Alloys Compd.*, 2017, **695**, 1743-1752.
18. Y. Lai, W. Liu, J. Li, K. Zhang, F. Qin, M. Wang and J. Fang, High performance sodium storage of Fe-doped mesoporous anatase TiO_2/amorphous carbon composite, *J. Alloys Compd.*, 2016, **666**, 254-261.
19. H. Liao, L. Xie, Y. Zhang, X. Qiu, S. Li, Z. Huang, H. Hou and X. Ji, Mo-doped Gray Anatase TiO_2 : Lattice Expansion for Enhanced Sodium Storage, *Electrochim. Acta*, 2016, **219**, 227-234.
20. F. Zhao, B. Wang, Y. Tang, H. Ge, Z. Huang and H. K. Liu, Niobium doped anatase TiO_2 as an effective anode material for sodium-ion batteries, *J. Mater. Chem. A*, 2015, **3**, 22969-22974.
21. D. Yan, C. Yu, Y. Bai, W. Zhang, T. Chen, B. Hu, Z. Sun and L. Pan, Sn-doped TiO_2 nanotubes as superior anode materials for sodium ion batteries, *Chem Commun (Camb)*, 2015, **51**, 8261-8264.
22. B. Liu, J. Wang, J. Li, K. Fan, D. Zhao, G. Liu, C. Yang, H. Tong and D. Qian, N-doped carbon coated TiO_2 hollow spheres as ultralong-cycle-life Na-ion battery anodes, *J. Phys. Chem. Solids*, 2019, **134**, 214-224.
23. S. Guan, Q. Fan, Z. Shen, Y. Zhao, Y. Sun and Z. Shi, Heterojunction TiO_2@$TiOF_2$ nanosheets as superior anode materials for sodium-ion batteries, *J. Mater. Chem. A*, 2021, **9**, 5720-5729.
24. P. Wang, X. Lu, Y. Boyjoo, X. Wei, Y. Zhang, D. Guo, S. Sun and J. Liu, Pillar-free TiO_2/Ti_3C_2 composite with expanded interlayer spacing for high-capacity sodium ion batteries, *J. Power Sources*, 2020, **451**, 227756.
25. Y. Wang, N. Li, C. Hou, B. He, J. Li, F. Dang, J. Wang and Y. Fan, Nanowires embedded porous TiO_2@C nanocomposite anodes for enhanced stable lithium and sodium ion battery performance, *Ceram. Int.*, 2020, **46**, 9119-9128.
26. H. Xu, W. Wang, G. Yu, L. Qin, Y. Jiang, L. Ren and J. Chen, Nitrogen-Doped Carbon-Coated TiO_2/TiF_3 Heterostructure Nanoboxes with Enhanced Lithium and Sodium Storage Performance, *ACS Appl. Energy Mater.*, 2020, **3**, 4738-4745.
27. J. Chen, E. Wang, J. Mu, B. Ai, T. Zhang, W. Ge and L. Zhang, CNTs–C@TiO_2 composites with 3D networks as anode material for lithium/sodium ion batteries, *J. Mater. Sci.*, 2019, **54**, 592-604.